Hyperfine Interact
DOI 10.1007/s10751-015-1168-2

Characterization of natural zeolite clinoptilolite for sorption of contaminants

E. Xingu-Contreras[1] · G. García-Rosales[1] · I. García-Sosa[2] · A. Cabral-Prieto[2] · M. Solache-Ríos[2]

Abstract The nanoparticles technology has received considerable attention for its potential applications in groundwater treatment for the removal of various pollutants as Cadmium. In this work, iron boride nanoparticles were synthesized in pure form and in presence of homo-ionized zeolite clinoptilolite, as support material. These materials were used for removing Cd (II) from aqueous solutions containing 10, 50, 100, 150, 200, 250, 300 and

Proceedings of the 14th Latin American Conference on the Applications of the Mössbauer Effect (LACAME 2014), Toluca, Mexico, 10–14 November 2014.

✉ E. Xingu-Contreras
nyleve_18@hotmail.com

G. García-Rosales
gegaromx@yahoo.com.mx

I. García-Sosa
irma.garcia@inin.gob.mx

A. Cabral-Prieto
agustin.cabral@inin.gob.mx

M. Solache-Ríos
marcos.solache@inin.gob.mx

[1] Instituto Tecnológico de Toluca, Avenida Tecnológico S/N, Fraccionamiento. La Virgen, C. P. 52149, Metepec, Estado de México, México

[2] Departamento de Química, Instituto Nacional de Investigaciones Nucleares, Apdo. Postal 18-1027, Col. Escandón, Deleg. M. Hidalgo, C. P. 11801, México D. F., México

Published online: 08 May 2015

400 mg/L. The characterization of these materials was made by using X-ray Diffraction, Scanning Electron Microscopy and Mössbauer Spectroscopy. Pure iron boride particles show a broad X-ray diffraction peak centered at 45° (2θ), inferring the presence of nanocrystals of Fe_2B as identified from Mössbauer Spectroscopy. The size of these Fe_2B particles was within the range of 50 and 120 nm. The maximum sorption capacities for Cd (II) of iron boride particles and supported iron boride particles in homo-ionized zeolitic material were nearly 100 %. For homo-ionized zeolite and homo-ionized zeolite plus sodium borohydride was $\geq$ 95 %.

Keywords Natural zeolites · Nanomaterials · Mössbauer spectroscopy · Sorption

1 Introduction

The presence and distribution of heavy metals such as Cadmium (Cd) is one of the environmental and public health more important problem today [1], because it is considered as a toxic element for humans as it is not biodegradable and tends to accumulate in living cells causing severe diseases and disorders [2]. The Agency for Toxic Substances and Disease from the United States lists Cd as the number six of most hazardous industrial wastes [3]. Currently, nanoparticles are a versatile mean for the removal of contaminants, first because of their small particle size (1–100 nm) and secondly because they can efficiently be transported by a flow of water so it may be injected under low pressure remaining in suspension for long periods of time [4]; the use of iron nanoparticles is one of the most promising techniques because they may act as a reducing and adsorber agents, among other properties; in addition to this, iron is inexpensive, non-toxic and environmentally compatible [5, 6]. Iron nanoparticles tend to agglomerate during preparation decreasing the reactivity of the particles as well as a poor mobility and subsequently then unsuccessful transport of iron nanoparticles [7]. Hence, loading pure iron or iron-coated nanoparticles onto supporting materials may be a potential method to decipher the agglomeration and sorption problems [8]. Literature reports mention the use of iron nanoparticles supported on various materials such as clays [9, 10], sawdust [11], activated carbon [12, 13], natural [14] and synthetic zeolites [15, 16] for removal of contaminants. Zeolite is an abundant natural resource and it has been used in the removal of heavy metals [17–19]. Thus the present study aims to use a Mexican natural zeolite Clinoptilolite, as a support material for iron nanoparticles, prepared by chemical reduction of an iron salt using sodium borohydride to study the sorption capacity of Cd (II) in aqueous solutions.

2 Experimental

2.1 Samples preparation

Natural zeolite clinoptilolite, from San Luis Potosí, México (ZC); was used to remover Cd (II) and at the same time as supporting material of iron boride nanoparticles. Natural zeolite was crushed and sieved using a 100 mesh. This sieved material was homo-ionized, i. e. treated with Na^{+1} ions to exchange them for cations such as Ca^{2+}, Mg^{2+} and K^{+} contained in the original zeolite. This material is identified as the homo-ionized zeolite clinoptilolite (HZC). The iron boride nanoparticles (IBNs) were synthesized by chemical reduction in an

inert atmosphere [20]. 0.07 M of $FeCl_3.6H_2O$ was dissolved in a mixture of ethanol/water in a ratio of 4/1 (v / v) (24 mL of ethanol for 6 mL deionized water), then 1 g of HZC was dispersed in this solution by stirring, 100 mL of a 0.1 M solution of $NaBH_4$ was added drop wise to this mixture. An excess of borohydride was added to complete the reaction. The produced black particles were separated by using the vacuum filtration technique. The solid particles were washed twice with 25 mL of absolute ethanol to remove all traces of water molecules and excess of $NaBH_4$. Finally the black particles were dried at 323 K for 12 h and they presented magnetism suggesting the presence of iron. This product was identified as: HZC-IBNs.

An experiment was carried out in order to see if there exist an influence of the $NaBH_4$ conditioning process on the sorption capacity of the HZC; for this purpose 100 mL of 0.1 M $NaBH_4$ solution were added drop wise to 1 g of HZC maintaining a continuous stirring. The resulting product was dried at 323 K for 12 h, this product was identified HZC-$NaBH_4$.

2.2 Samples characterization

The characterization of the different materials was as follows: X-ray Diffraction (XRD) patterns of the IBNs and HZC-IBNs materials were recorded by using a Siemens® D5000 diffractometer with Cu Kα radiation and a mono-chromated beam. The X-ray tube was operated at 35 kV and 20 mA.

The elemental composition of the HZC, HNZ-NaBH4, IBNs and HZC-IBNs materials was determined by using a Scanning Electron Microscopy (SEM), a JEOL® JSM 500 LV apparatus with an Energy Disperse X-ray Spectroscopy (EDS) system.

The samples containing iron (ZC, HZC, HZC-IBNs) were analyzed by Mössbauer spectroscopy (MS) using a Wissel® constant acceleration spectrometer with a $^{57}Co/Rh$. The reported isomer shifts are referred to that of metallic iron.

2.3 Sorption isotherms

The sorption tests of Cd (II) were carried out by using a batch system, which consisted on leaving in contact 100 mg of a chosen sample: HZC, HZC-$NaBH_4$, IBNs or HZC-IBNs in 10 mL of solutions of cadmium nitrate, Cd $(NO_3)_2$ $4H_2O$, with concentrations of 10, 50, 100, 150, 200, 250, 300 and 400 mg Cd/L. Each mixture was put in vial and the vials were put in a shaker at 120 rpm at 303 K for 24 h. Subsequently the separation of the liquid phase was carried out by centrifugation. The analysis of the liquid phase was performed by atomic absorption spectrophotometry in a GBC® 932 PLUS equipment for the determination of Cd (II) (at wavelength 331.1 nm). All experiments were carried out twice for consistency.

3 Results and discussion

3.1 XRD

Figure 1 shows the XRD patterns of IBNs and HZC-IBNs materials. Figure 1a shows a broad peak at 45° (2θ) indicating the presence of very small crystals or amorphous material. According to the expected reaction products, Fe and Fe_2B may be present [21]. From such a peak broadness it is impossible to discern between these end-products because both show a diffraction peak around 45° (2θ), Mustapic et al. [21] suggest that this broad pattern may be associated directly to Fe_2B, which will be confirmed later on by Mössbauer spectroscopy.

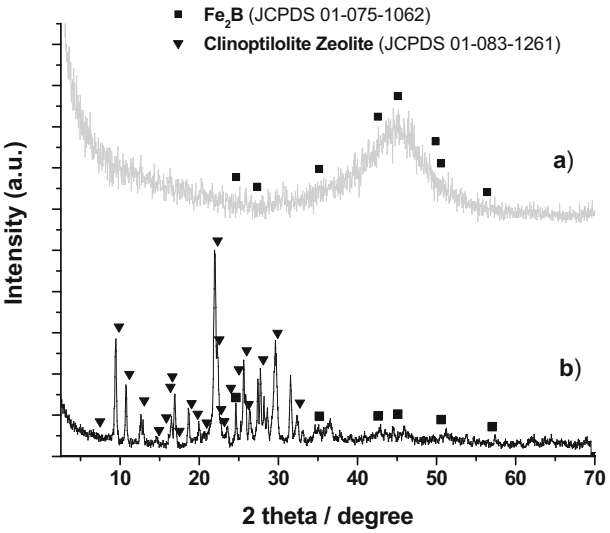

Fig. 1 Powder x-ray diffractogram: **a** IBN and **b** HZC-IBNs

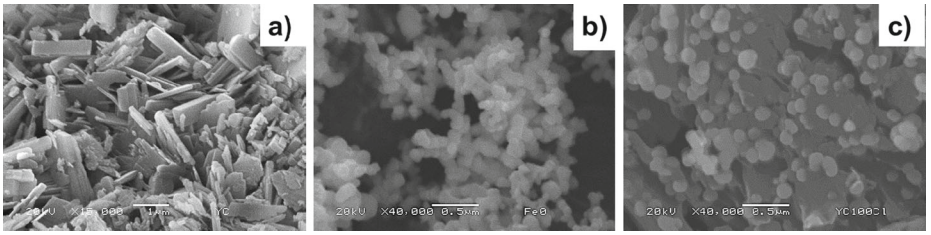

Fig. 2 SEM images: **a** HZC, **b** IBNs and **c** HZC-IBNs

The XRD pattern of the HZC-IBNs material is shown in Fig. 1b and it was compared with JCPDS data cards of clinoptilolite (01-083-1261) and Fe_2B (01-075-1062). This comparison suggests that there were not any visible changes in the structure of clinoptilolite after the iron-boride nanoparticles were supported. On the other hand, the presence of the IBNs can not be distinguished clearly from this pattern because the low intensity and their low crystal size. Their presence was simply confirmed by the black color of the end-product and its magnetism.

3.2 SEM

3.2.1 Morphology

The presence of large tabular crystals after the homo-ionization process with Na^{+1} ions is typical of the clinoptilolite zeolite as observed from Fig. 2a [17, 19, 22]. On the other hand, Fig. 2b shows the IBNs synthesized in this work; it can be observed that these nanoparticles are spherical having particle sizes from 50 to 100 nm. Agglomeration of the IBNs occurs due to the magnetic properties mainly [21, 23]. This agglomeration decreases considerably

Table 1 Elemental analysis of materials

Elements	ZC W %	HZC W %	HZC − $NaBH_4$ W %	IBNs W %	HZC − IBNs W %	HZC + Cd W %	HZC − $NaBH_4$ + Cd W %	IBNs + Cd W %	HZC − IBNs + Cd W %
Na	0.57(0.04)	3.17(0.11)	3.24(0.16)	ND	2.53(0.09)	1.54(0.10)	1.96(0.14)	ND	1.22(0.18)
Mg	0.15(0.03)	0.17(0.05)	0.08(0.06)	ND	ND*	ND	ND	ND	ND
K	1.74(0.09)	1.31(0.10)	1.82(0.12)	ND	0.85(0.15)	ND	ND	ND	ND
Ca	2.63(0.17)	0.67(0.02)	0.85(0.09)	ND	0.47(0.08)	ND	ND	ND	ND
Fe	1.04(0.06)	0.92(0.11)	1.57(0.11)	91.7(0.71)	32.09(5.65)	1.61(0.14)	1.60(0.12)	66.72(0.79)	22.70(11.96)
O	46.03(0.12)	45.85(0.05)	46.72(0.22)	8.3(0.71)	27.96(0.14)	46.84(0.34)	45.95(0.10)	28.88(0.88)	38.14(5.08)
Si/Al	4.25(0.43)	4.78(0.21)	4.95(0.18)	ND	4.23(0.13)	4.88(0.18)	4.79(0.16)	ND	4.74(0.30)
Cd	ND	ND	ND	ND	ND	5.12(0.23)	5.22(0.23)	4.40(0.28)	7.21(1.24)

(*)ND -not detected, the numbers inside the parenthesis are the standard deviations.

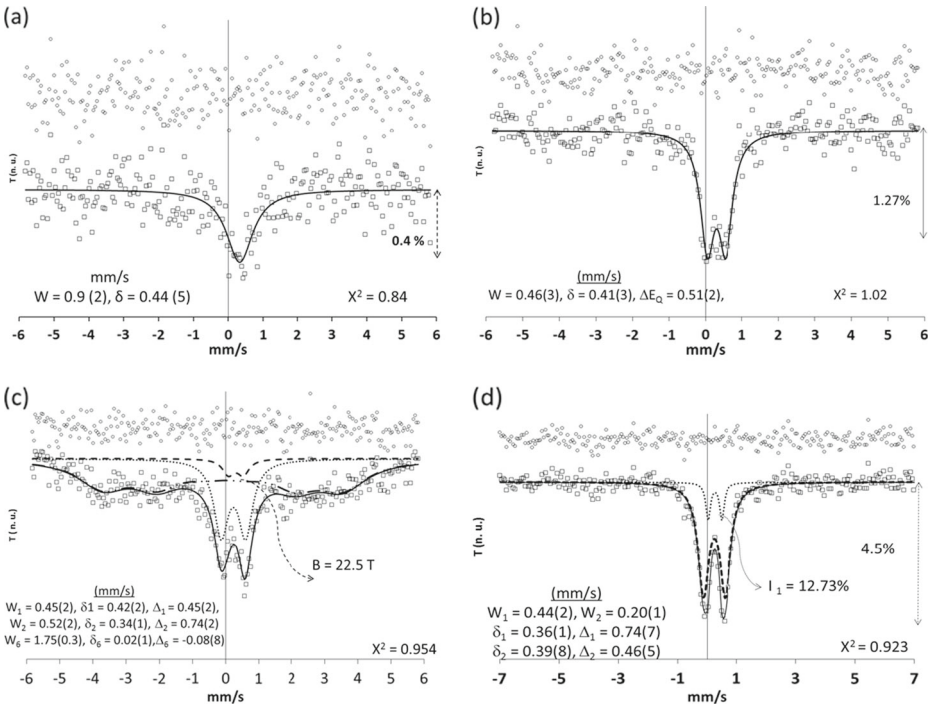

Fig. 3 Mössbauer spectra of: **a** ZC, **b** HZC, **c** HZC-IBNs, **d** after removal of Cd (II) with HZC-IBNs+Cd

when these IBNs are supported in the homo-ionized zeolite, Fig. 2c; it can be seen from this figure the spherical particles with diameters ranging from 60 to 120 nm.

3.2.2 Sample elemental composition

The chemical composition of the samples ZC, HZC, HZC-$NaBH_4$, IBNs and HZC-IBNs, was determined by EDS before and after the sorption process of Cd (II) as presented in Table 1. The HZC material presents a significant amount of Na after the homo-ionization process; see columns two and three of Table 1. Fe was found in the natural zeolite, and it can be considered as part of the zeolite structure [24, 25] or as an impurity. For the sample HZC-$NaBH_4$ the Na content after putting in contact the zeolite with $NaBH_4$ remained practically the same as in the original HZC, see column three and four of Table 1. The composition of the synthesized IBNs consists of iron and oxygen mainly, the low content of the oxygen can be associated to oxidation of the nanoparticles. The Fe content in the mixed HZC-IBNs material increased due to the presence of the iron boride nanoparticles. The data concerning the sorption process of Cd will be discussed in the sorption isotherms section.

3.3 Mössbauer spectroscopy

Figure 3 shows the Mössbauer spectra of the ZC, HZC, HZC-IBNs and HZC-IBNs+Cd samples. The Mössbauer spectrum of the natural zeolite, Fig. 3a shows a broad singlet indicating the presented iron whose hyperfine parameter is $\delta = 0.44(5)$ mm/s. A quadrupole doublet could be fitted but the resulting standard deviation ($\sigma = 0.48$) of the quadrupole

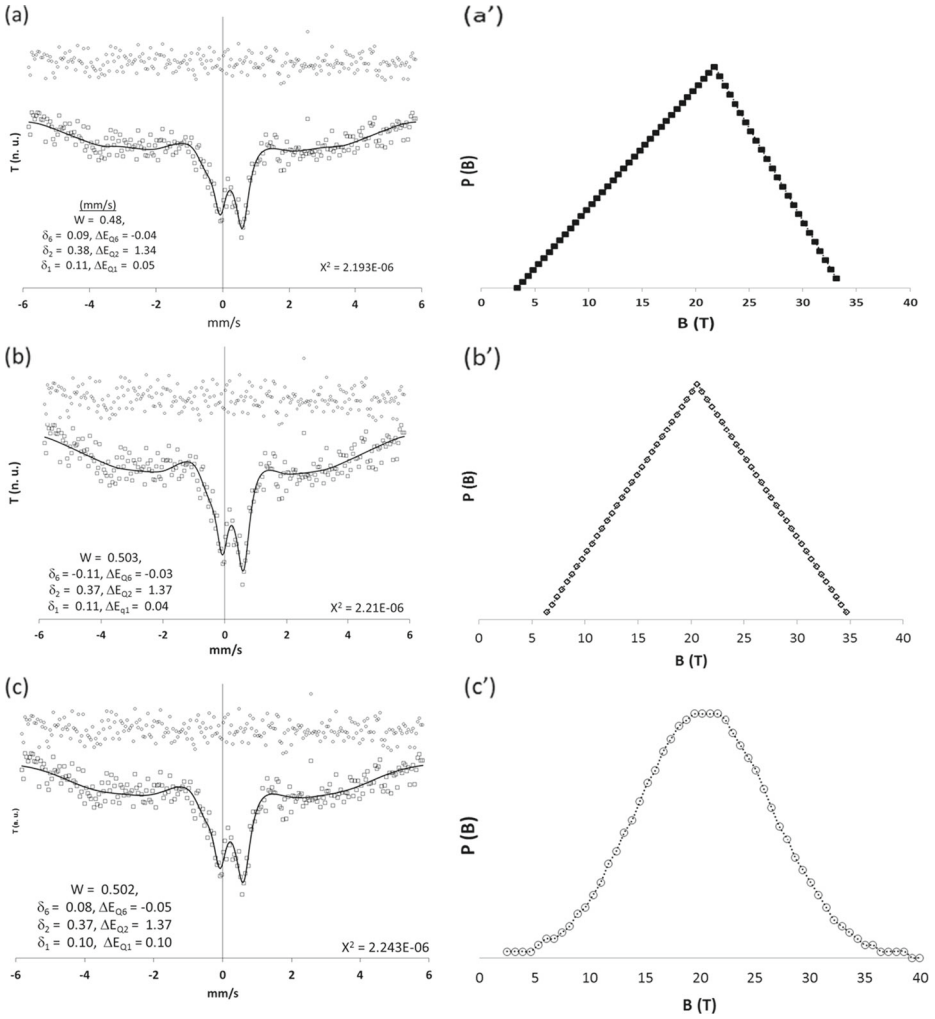

Fig. 4 Mössbauer spectrum of HZC + IBNS (a, b, c) and analyzed with **a'** an asymmetrical triangular; **b'** a triangular and **c'** a Gaussian hyperfine field distribution functions

splitting, $\Delta E_Q = 0.24$ mm/s, is twice its value ignoring for this reason the presence of such a doublet. Thus the presence of iron in the clinoptilolite zeolite is probably located in distorted tetrahedral sites as indicated by Bish and Boak [24] and Breck [25]. The Mössbauer spectrum of the HZC sample presents a quadrupole doublet as shown in Fig. 3b. The transmission Mössbauer effect increases from the untreated to the homo-ionized zeolite. Figure 3c shows, on the other hand, the resulting Mössbauer spectrum of the iron boride nanoparticles supported in HZC, see the SEM image of this sample in Fig. 2c. This Mössbauer spectrum could be fitted with two quadrupole doublets: one of them belonging to iron in the natural zeolite with a relative intensity of 4.42 % and the other with a relative intensity of 26.2 %, and a magnetic pattern having a hyperfine magnetic field $B = 22.45$ T with a relative intensity of 69.37 %. All these patterns present broad lines as seen from the

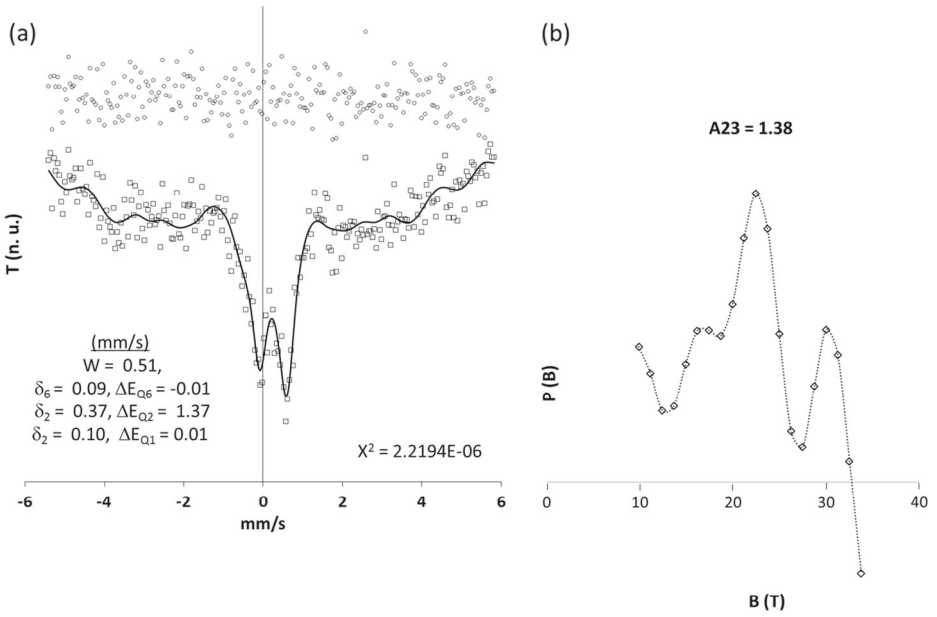

Fig. 5 **a** Fitted Mössbauer spectrum using the non-implicit distribution $P(B) = (aCos(\pi B) + bSin(\pi B))^n$ [31], **b** multi-modal distribution

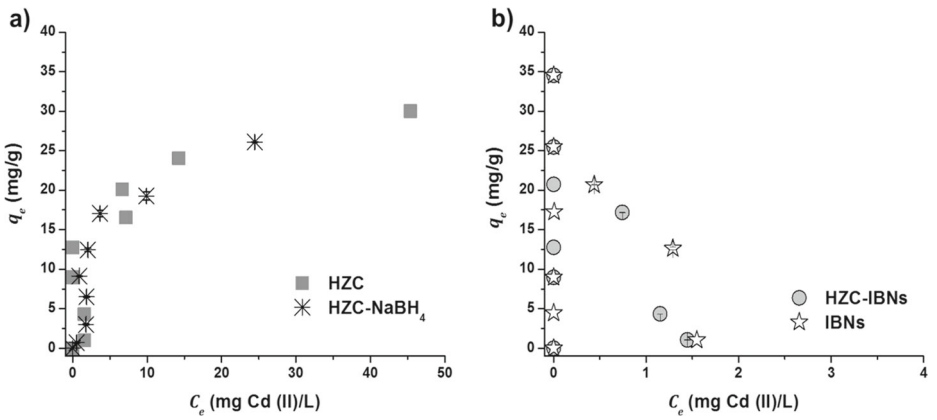

Fig. 6 Isotherm of concentration of Cd (II): **a** HZC and HZC-$NaBH_4$, **b** IBNs and HZC-IBNs

inset numbers of Fig. 3c. The estimated discrete value of the hyperfine magnetic field from this spectrum ($B = 22.45$ T) could be associated with an iron boride or various iron borides [26]. From the Mössbauer parameters of the most intense quadrupole doublet ($I_2 = 26.\ \%$), observed in Fig. 3c one can infer an oxidation process on the IBNs surface; the broad line width of this doublet may also suggests that more than one iron oxide is produced [27]. After the sorption process of Cd (II) in the HZC-IBNs sample which was allowed to dry under atmospheric conditions, the powder turns from black to ochre and the resulting Mössbauer

Table 2 Adsorption isotherm parameters of Cd (II) for HZC, HZC − $NaBH_4$, IBNs and HZC-IBNs

Material	Langmuir	Freundlich	Langmuir-Freundlich
HZC	$q_e = 32.780$ (mg/g) $b = 0.120$ $R^2 = 0.822$	$K = 6.587$ $n = 2.372$ $q_e = 31.090$ (mg/g) $R^2 = 0.768$	$K = 1.595$ $n = 1.718$ $a = 0.053$ $q_e = 29.400$ (mg/g) $R^2 = 0.838$
HZC − $NaBH_4$	$q_e = 27.680$ (mg/g) $b = 0.218$ $R^2 = 0.933$	$K = 6.710$ $n = 2.276$ $q_e = 35.760$ (mg/g) $R^2 = 0.916$	$K = 6.323$ $n = 0.905$ $a = 0.220$ $q_e = 25.120$ (mg/g) $R^2 = 0.933$
IBNS	Not applicable*	Not applicable*	Not applicable*
HZN-IBNS	Not applicable*	Not applicable*	Not applicable*

(*) in these systems almost a 100 % of Cd (II) was removed from any studied solution.

spectrum is a broad quadrupole doublet as shown in Fig. 3d whose Mössbauer parameters are : W = 0.44 mm/s, $\delta = 0.36$ mm/s, and $\Delta = 0.68$ mm/s. This broad doublet can be fitted to two quadrupole doublets, whose Mössbauer parameters may be characteristic of ferrihydrite [28–30]. This iron hydro-oxide compound is inferred due the oxidation of iron boride nanoparticles. Low temperature measurements should assess the nature of this broad quadrupole doublet completely.

While analyzing the broad magnetic pattern in Fig. 3c using different hyperfine magnetic field distributions (HMFDs) one obtains the following results. The resulting implicit HMFDs are shown in Fig. 4a', b', c'. The asymmetric distribution function gives the best numerical result. Interestingly the worst solution is given by the Gaussian distribution function.

On the other hand, from such distributions one may discard the presence of pure, Fe^0, which is confirmed by looking at the HMFD obtained from a non-implicit trigonometric function [31].

One can observe from Fig. 5b that three well defined peaks appear in the HMFD function suggesting different iron phases. The suggested hyperfine fields given by this distribution are 17, 22 and 30 T instead of a distribution with a single maximum as shown in Fig. 4. It can be inferred from both, Figs. 4a, b, c and 5a, that pure iron particles are not present. Thus present Mössbauer analysis suggests that the spherical nanoparticles, shown in Fig. 2c, consist of spherical iron-boride particles (Fe_2B) [32] covered with an iron oxide shell characterized by parameters δ_2, ΔE_{Q2}, W_2. The EDS analysis did showed an $\sim$ 8W % of oxygen from any of the analyzed spherical particles.

4 Sorption isotherms

Figure 6 a and b show the relationship between residual concentrations (C_e) and sorption capacities (q_e) of each sorbent. According to Fig. 6a the HZC and HZC-$NaBH_4$

materials provide the typical sorption behavior reaching practically the plateau at the maximum studied concentrations. For the IBNs and HZC-IBNs materials this sorption behavior was different. In these cases, Fig. 6b, the sorption of Cd(II) is almost complete at any studied concentration, i. e. the sorption capacity was > 95 %. One can observe from Fig. 6b the q_e values for every initial concentration (C_i) by looking at the symbols; those lying on the Y-axis indicate complete sorption and those at the right hand side of the Y-axis suggest an un-complete sorption, although the capacity sorption is still > 95 %.

The sorption isotherms of Fig. 6a were analyzed by using Langmuir, Freundlich and Langmuir-Freundlich equations using Statistica 7 free software package and the obtained parameters are shown in Table 2. It was found that the best fitting was when using the Langmuir-Freundlich model. Its correlation coefficient was higher than the values of the Langmuir and Freundlich models. Generally speaking, an average value can, however, be considered from all calculated q_e values since there is not a significant difference among these three models. Accepting this, the average values are: 31.09 mg/g for HZC and 29.52 mg/g for HZC-$NaBH_4$, suggesting almost the same sorption capacity between these materials. In this sense the $NaBH_4$ does not influence the sorption process of Cd (II) in the zeolite.

In this work, the sorption capacity for the HZC material is higher than in previous reports, for example, by Cortés-Martínez [18] and by Teutli-Sequeira [19]. These differences could be attributed to a different origin of the clinoptilolite zeolites.

On the other hand, the Na content of HZC and HZC-$NaBH_4$ materials before the sorption process of Cd are 3.14 and 3.24 W %, respectively, Table 1. After the sorption process of Cd the sodium content was 1.54 and 1.96 W %, respectively. Such a decrease on the Na content after the sorption of Cd suggests that there was a cation exchange mechanism besides the physical sorption. This decrease in the Na content is also observed in the HZC-IBNs material to 1.22 W % (column 10 of Table 1), therefore the cation exchange mechanism is also involved in this material. Furthermore, the HZC-IBNs remove 5mg/g more than the HZC material alone, suggesting an additional mechanism associated with the IBNs. On the other hand, the IBNs alone remove a similar amount of Cd than the HZC-IBNs material, see Fig. 6b. In this case the sorption mechanism of Cd takes place on the surface of the IBNs [33–35]. Some authors suggest physical sorption, chemi-sorption or surface complexation [33]; other authors consider a diffusion process on the surface particles and inter-particles or pore diffusion [34]. Even more, a reduction process of Cd or other metals by iron nanoparticles has also been considered [33, 35]. In our case, we can suggest an oxidation process in the IBNs as indicates the data of Table 1. For instance, the elemental composition of the initial IBNs is the following: 91.7 W % is associated with the iron content and the rest of 8.3 W % is associated with oxygen. The EDS analysis cannot detect boron. After the sorption process of Cd in the IBNs+Cd system, the elemental analysis for Fe, O and Cd was 66.72, 28.88 and 4.4 W %, respectively. The high content of oxygen after the sorption process indicates then an oxidation reaction. A precise chemical species of Cd require more studies, particularly XPS analysis.

5 Conclusions

In this study, iron boride nanoparticles were synthesized by chemical reduction and were also supported in homo-ionized natural zeolite clinoptilolite to remove Cd (II). Whereas the size of the IBNs in its pure form was between 50 and 100 nm and in the supported form was between 60 and 120 nm. These IBNs were identified as Fe_2B from MS mainly. The

sorption capacities of Cd of HZC, HZC-$NaBH_4$, IBNs and HZC-IBNs, were in the same order of magnitude although the HZC, HZC-$NaBH_4$ materials removed Cd following a normal isotherm sorption that could be represented by the combined Langmuir-Freundlich model, suggesting a heterogeneous material. The maximum sorption capacity of these both materials was around 30 mg/g. The IBNs and HZC-IBNs systems did not follow any of the studied sorption models but their sorption capacities was 35 mg/g, a little higher than the previous materials. It would be interesting to determine the maximum sorption capacities of IBNs and HZC-IBNs for Cd, since they were not reached in the experimental conditions of this work. Boparai et al. [34] report sorption capacities up to $\sim$ 770 mg/g at 297 K.

References

1. Purkayastha, D., Mishra, U., Biswas, S.: J. Water Process Eng. **2**, 105 (2014)
2. Pérez-García, P.E., Azcona-Cruz, M.I.: Rev. De Especialidades Médico-Quirúrgicas **17**(3), 199 (2012)
3. U.S. Department of Health and Human Services Public Health Service Agency for Toxic Substances and Disease Registry www.atsdr.cdc.gov
4. Pandipriya, J., Praveena, E., Kuriakose, R.M., Suganiya, Marcilin, J.A., Magthelin, T., Nandhitha, N.M.: Int. J. Eng. Res. Appl. (Version 1) **4**(4), 203 (2014)
5. Zhang, W., Elliot, D.W.: Remediat. J. **16**, 7 (2006)
6. Junyapoon, S.: KMITL Sci. Technol. J. **5**(3), 587 (2005)
7. Schrick, B., Hydutsky, B.W., Blough, J.L., Mallouk, T.E.: Chem. Mater. **16**, 2187 (2004)
8. Cumbal, L., Greenleaf, J., Leun, D., SenGupta, A.K.: React. Funct. Polym. **54**, 167 (2003)
9. Li, S., Wu, P., Li, H., Zhu, N., Li, P., Wu, J., Wang, X., Dang, Z.: Appl. Clay Sci. **50**, 330 (2010)
10. Frost, R.L., Xi, Y., He, H.: J. Colloid Interface Sci. **341**, 153 (2010)
11. Sánchez, N., Vazquez, M., Torresi, R. Revista Facultad de Ingeniería Universidad Antioquia **55**, 18 (2010)
12. Behrooz-Zargar, Hooshang-Parham, Monir-Rezazade: J. Chin. Chem. Soc. **58**, 694 (2011)
13. Zhu, H.J., Jia, Y.F., Yao, S.H., Wu, X., Wang, S.Y.: China Environ. Sci. **30**(12), 3562 (2009)
14. Naderpour, H., Noroozifar, M., Khorasani-Motlagh, M.: J. Iran. Chem. Soc. **10**, 471 (2013)
15. Wahyuni, E., Arryanto, Y., Setiadji, B., Webb, J., Chua-Anusorn, W.: Adsorpt. Sci. Technol. **8**, 653 (2000)
16. Wang, W., Zhou, M., Mao, Q., Yue, J., Wang, X.: Catal. Commun. **11**(11), 937 (2010)
17. Leyva-Ramos, R., Berber-Mendoza, M.S., Mendoza-Barrón, J., Aragón-Piña, A.: J. Chem. Soc. **48**(2), 130 (2004)
18. Cortés-Martínez, R.: Thesis to obtain the degree PhD in water sciences. UAEM (2007)
19. Teutli-Sequiera, A., Solache-Ríos, M., Olguín, M.T.: Hydrometallurgy **97**, 46 (2009)
20. Yuvakkumar, R., Elango, V., Rajendran, V., Kannan, N.: Dig. J. Nanomater. Biostructures **6**(4), 1771 (2011)
21. Mustapic, M., Pajic, D., Novosel, N., Babic, E., Zadro, K., Cindrié, M., Horvat, J., Skoko, Z., Bijelic M., Shcherbakov, A.: Croat. Chem. Acta **83**(3), 275 (2010)
22. Tsitssihvili, G.V., Andronikashvili, T.G., Kirov, G.R., Filizova, D.: Natural Zeolites. Ellis Horwood Limited, England (1991)
23. Bhowmick, S., Chakraborty, S., Mondal, P., Van Renterghem, W., Van den Berghe, S., Roman-Ross, G., Chatterjee, D., Iglesias, M.: Chem. Eng. J. **243**, 14 (2014)
24. Bish, D.L., Boak, J.M.: Clinoptiliolite-heulandite nomenclature. In: Bish, D., Ming, D.W. (eds.) Reviews in Mineralogy and Geochemistry, Mineralogy Society of America, vol. 45, p. 207 (2001)
25. Breck, D.W.: Zeolite Molecular Sieves. Structure, chemistry and use. Robert E. Krieger Publishing Company, Florida (1984)
26. Frank, H., Rosenberg, M.: J. Magn. Magn. Mater. **7**, 168 (1978)
27. Kumar, S., Layek, S., Pandey, B., Verma, H.C.: Int. J. Eng. Sci. Technol. **2**(8), 66 (2010)
28. Schütz, M.R., Schedl, A.E., Wagner, F.E.: Breu J. Appl. Clay Sci. **54**, 281 (2011)
29. Ohihiko, Y., Kawabata, T., Shishido, T., Takaki, K., Zhang, Q., Wang, Y., Nomura, K., Takehira, K.: Appl. Catal. A Gen. **288**, 220 (2005)

30. Kumbhar, P.S., Sanchez-Valente, J., Millet, J.M.M., Figueras, F.: J. Catal. **191**, 467 (2000)
31. Cabral-Prieto, A.: Hyperfine Interactions, vol. 224, p. 15 (2014)
32. Sánchez, F.H., Zhang, Y.D., Budnick, J.I., Hasegawa, R.: J. Appl. Phys. **66**(4), 1671 (1989)
33. Zhang, Y., Li, Y., Dai, C., Zhou, X., Zhang, W.: Chem. Eng. J. **244**, 218 (2014)
34. Boparai, H.K., Joseph, M., O'Carroll, D.M.: J. Hazard. Mater. **186**, 458 (2011)
35. Xi, Y., Mallavarapu, M., Naidu, R.: Mater. Res. Bull. **45**, 1361 (2010)